



First Principle Computational Study of the Electronic and Structural Properties of Lead Telluride (PbTe)

Adamu, M.A.*, Ahuome, B.A., Adamu, I., Baba-Kutigi, A.N.

Federal University Dutsin-Ma, Katsina State, Nigeria

*Corresponding Author: adamuaminu532@gmail.com

Abstract The electronic and structural properties of Lead Telluride (PbTe) compound were computed using FHI-aims DFT code. We first of all relaxed the structure by using Brillouin-zone of $12 \times 12 \times 12$ k-grids for the self-consistent field (SCF) convergence. For the exchange correlation functional, we used Perdew Burke Ernzerhof approximation. We obtained the most stable structure to be halite structure with total ground state energy of -777754.818 eV. The fundamental band gap was found to be 0.75632758 eV, similarly the DOS computations show a good availability of electronic states in the conduction band (CB) and valence band (VB). The research shows that PbTe is a promising material for solar cell as well as thermoelectric applications.

Keywords DFT, PbTe, Band Gap, Ground State Energy, PBE

1. Introduction

Interesting properties of IV-VI semiconductor compounds have become a subject of extensive research on the lead chalcogenides (also known as lead salt) PbX ($X = S, Se, Te$) [1-6]. The systematic and logical studies of such compounds on theoretical, computational as well as experimental background have provided fascinating properties which have wide technological applications [2]. Researchers have found out that the wide potential of these compounds as good semiconductor devices are due to their narrow band gap, high dielectric constant, high carrier mobility, positive temperature coefficient of the band gap, and negative pressure dependence of the band gap [2, 4-9]. As a result of such anomalous properties, they are applicable in the branches of thermoelectric, visible, gamma and infrared (IR) detectors and sensors [3-13]. More recently, they are also used as IR laser in fiber optics, super lattices, quantum dots and multiple exciton generation [6-7, 14-15]. On account of narrow band gap of ~ 0.31 eV at 300K [7-9, 13, 26] and high absorption coefficient [3, 13] of PbTe, it appeared to be a suitable candidate for applications in optoelectronic devices [12-13, 18-19]. It was also reported [2] that, the outstanding properties of PbTe and IV-VI semiconductor compounds as compared to III-V and II-VI semiconductors are due to the interaction of Pb s-electron valence band with the Te p-electrons valence band. Exceptional properties of this material were the motive to synthesize, compute and characterize their properties. In the last few decades, a number of studies on its deposition and characterization were reported; see for example, [11-13, 15-19].

Many researchers have used different types of deposition techniques to deposit PbTe thin film. For instance, [18] fabricated PbTe thin films with different thickness using vacuum technique. In [17], PbTe thin films growth on various substrate {glass, Si (100), Si (111), BaF_2 (111)} by pulsed laser deposition was reported. Similarly, [21] grew PbTe by hot wall epitaxy on BaF_2 substrates. In another report, [32] deposited PbTe thin films on a non-conducting glass substrate through solvo thermal method. PbTe thin films were also deposited by other methods such as magnetron sputtering, pulsed laser evaporation [21], vacuum evaporation method [8], flash evaporation method [7], two stage process, first stage using chemical bath deposition (CBD), and then chemical vapor deposition (CVD) [12-13].



Computational wise, many researchers who performed DFT computation of PbX properties are mentioned in Ref. [1]. However, [1] also computed the optical and electronic properties of Lead Chalcogenides using DFT-LDA/GGA, hybrid functional and GW. They show that hybrid functionals describe important aspects of the band structure of these materials which LDA/GGA clearly fail to describe. They performed their calculations using the projector augmented wave (PAW) method and the full potential (Linearized) augmented plane wave plus local orbital [FP-(L) APW+ LO] method. The results obtained by the PAW and the FP-APW+ LO methods take into account spin orbit coupling (SOC), and incorporate the semi core Pb 5d states as valence states. Hence, it is the aim of this study to systematically and logically compute the most stable electronic structure of PbTe using an all electron numeric atom-centered basis set that include both the core and valence electrons. Similarly, we also incorporate the SOC to account for the Pb and Te large atomic number.

2. Methodology

Density functional Theory code of Fritz Haber Institute for ab-initio molecular simulation was used for the computation. DFT requires the electron density of a material $n(\vec{r})$, to be self-consistently solved according to the Kohn-Sham equations which computes the energy E from $n(\vec{r})$;

$$E = \sum_i^N \epsilon_i - \frac{1}{2} \iint \frac{n(\vec{r}_1) n(\vec{r}_2)}{|\vec{r}_1 - \vec{r}_2|} d\vec{r}_1 d\vec{r}_2 + E_{xc}[n] - \int_{xc} V(\vec{r}) n(\vec{r}) d\vec{r} \quad (1.1)$$

$V_{xc}(\vec{r})$ is the exchange-correlation (xc) potential of atomic nuclei, $E_{xc}[n]$ is the xc energy functional, the double-integral provides the electron-electron interaction. $E_{xc}[n]$ serves as a correction for the errors in the kinetic energy functional and the electron-electron double-integral. In principle DFT is exact, the approximation is only in the xc energy and potential. One of the approximations for xc is the generalised gradient approximation (GGA) as parameterized by Perdew, Burke and Ernzerhof PBE. It gives the effective potential that depend both on the local density and its local gradient. The GGA approach therefore corrects the problems encountered in the local density approximation (LDA).

$$E_{xc}^{GGA}[n \uparrow n \downarrow] = \int \epsilon_{xc}[n \uparrow n \downarrow \nabla n \uparrow \nabla n \downarrow] n(\vec{r}) d(\vec{r}) \quad (1.2)$$

In this work, the total ground state energy of PbTe were calculated in the Generalized Gradient Approximation GGA using the PBE exchange-correlation energy functionals.

The calculation was performed by using Brillouin-zone of $12 \times 12 \times 12$ k-grids for the SCF convergence. We used a lesser k-space to integrate the DOS. The factors by which the original k-space from the SCF cycle is increased are now (5, 5, 5). Together with the original k-grid of $12 \times 12 \times 12$, this makes for a $60 \times 60 \times 60$ integration mesh that is used for the DOS. A Gaussian broadening of 0.05eV was used for the DOS computations. We used an experimental lattice constant of $a = 6.454 \text{ \AA}$ for the PbTe lattice parameters. Fig. 1.1 shows the crystalline structure of PbTe with Pb and Te represented by the bigger and smaller balls respectively.

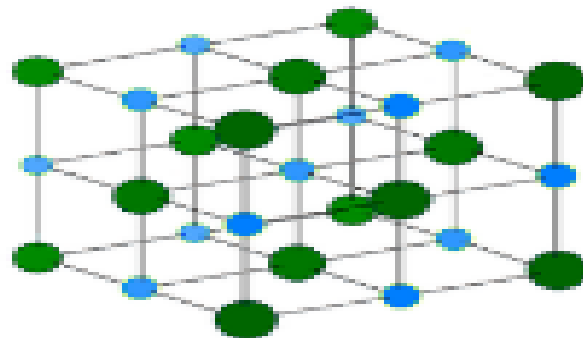


Figure 1: PbTe crystalline structure



In Fig. 1, PbTe crystalline lattice is presented. We optimize the geometry using $1e^{-4}$ eV, while for the unit cell we select the full relaxation option. For this optimized geometry, we obtain the following three lattice vectors and atomic coordinates as shown in Table 1.

Table: 1

Crystal structure	Atomic coordinates (\AA)			Lattice vectors (\AA)			
Fcc	-0.0021	-0.0021	-0.0021	Pb	3.2387	3.2387	-0.0116
	3.2291	3.2291	3.2291	Te	-0.0116	3.2387	3.2387
					3.2387	-0.0116	3.2387

3. Results

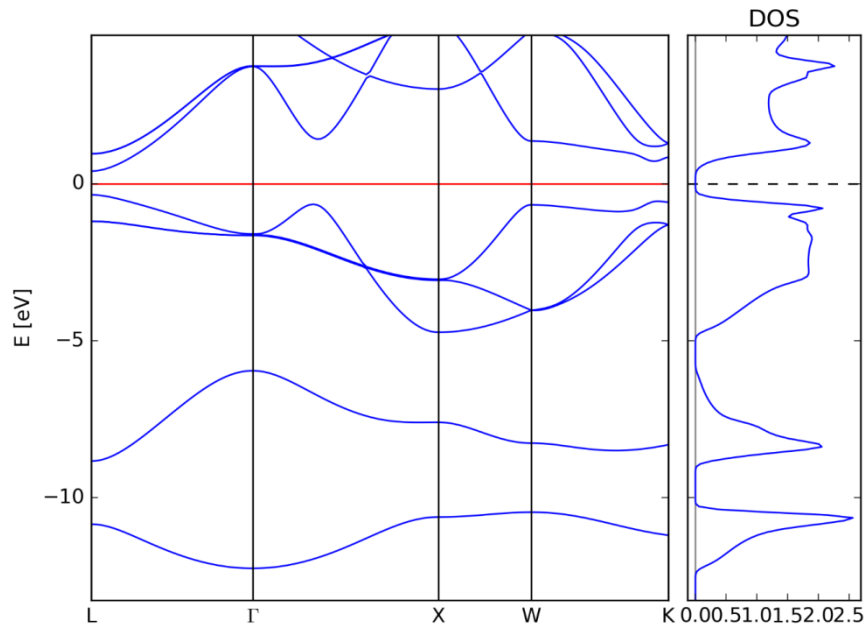


Figure 2: The Band structure and DOS of PbTe

The results obtained are based on the output files from the FHI-aims code used for simulation. The optimized PbTe structure and its parameters were used to calculate the DOS, band structure, Ground state energy, HOMO, LUMO and the HOMO-LUMO gap.

Figure 2 shows the PbTe band structure and DOS. The mini gap for PbTe appears at L- symmetry point resulting from pushing the anion p states upward, this occurs between -5.089 eV (valence) and -4.333 eV (conduction). Since states with equal symmetry repel each other, this gives rise to strong level repulsion, which determines the main features of the band structures and is the origin of their peculiarities [1]. Since the HOMO and LUMO are on the same symmetry point, our work shows that PbTe is a direct band gap semiconductor. Moreover, the LUMO bottom indicate an s-like atom character which is localized on an anion splits off from the rest of the valence band antisymmetric gap, and p-like around the group VI (Te). This difference is relevant, it is use in interpreting Knight-shift data and the temperature dependence of band states [42].

Table 2: Fundamental Direct Band gap of PbTe

Crystal structures	HOMO (VBM) (eV)	LUMO (CBM) (eV)	HOMO-LUMO gap (eV)	Total Energy (eV)	Other research Band gap (eV)
PbTe	-5.08988074	-4.33355316	0.75632758	777754.818	0.3[32,36], 0.7[1]



This again gives rise to a difference in the nature of the HOMO and LUMO which retards the return of the excited electron to the valence band. However, it makes the state near the valence band maximum have p bonding character which are associated with more electronegative element in the solid, while those near the conduction band minimum have p anti-bonding character and are associated with less electro negativity. The main effect on the band structure due to SOC is that the topmost valence band is shifted upward, whereas the lowest conduction band is moved downward in energy, resulting in a significant reduction of the direct energy gap at the L point.

The energy band gap is seen as the difference between the conduction band and the valence band which is estimated to be 0.76 eV as shown in Table 1. This value is in good agreement with the value computed by [1] using PBE. However, the experimental value of the direct band gap is 0.31 eV as obtained by [32, 36]. This is so because, standard DFT-PBE largely overestimates the band gap in PbTe [1].

Figure.2: also shows the Density of state of PbTe as a halite structure semiconductor; we divide the density of state into three general regions while analysing. The first region is the most tightly bound energy band where electron states corresponding to this band are strongly localized on the anion state. The next region of noticed is a peak arising from the onset of the second valence band which shows there is no energy variation along the symmetry direction; in fact, it is very flat over the entire square face of the Brillouin zone. The character of state associated with the second valence band changes from predominantly cation s-like states at the band edge to predominantly anion p-like state at the band maximum. The third region of interest in the density of state extends from the onset of the third valence band to the valence band maximum. This region encompasses the top two valence bands and is predominantly p-like and is associated with anion state.

4. Conclusion

This work has successfully employed DFT-PBE functional method to calculate and estimate the band structure and DOS of PbTe using FHI-aims in which the input parameters are optimized. The minimum total energy obtained from the experimental lattice constant of 6.454 \AA results in -777754.818 eV . The calculated electronic band structure show that PbTe is a direct band gap semiconductor with 0.75 eV HOMO-LUMO gap. The DOS energy level within the semiconductors shows considerable high state of electron occupation and the DOS observed around the Fermi level for the semiconductors at zero level indicate that they have conducting properties. In general, FHI-aims code has predicted the band structure and DOS calculation within a reasonable computational time when compared to some other DFT theoretical programs observed in literature.

Acknowledgement

Our special gratitude goes to Tertiary Education Trust Fund (TET Fund) for the support through her Institutional Base Research (IBR) sponsorship programme.

References

- [1]. Kerstin H., Andreas G., and Georg K. (2007), Structural and electronic properties of lead chalcogenides from first principles. *Physical Review B* 75, 195211, PACS number(s): 71.15.Mb, 71.20.Nr, DOI: 10.1103/PhysRevB.75.195211
- [2]. Bhambhani, P., Kabra, K., Sharma, B.K. and Sharma, G. (2014) High Pressure Study of Structural and electronic Properties of PbSe, *Journal of Solid State Physics*, <https://doi.org/10.1155/2014/921092>.
- [3]. Munoz, V., Lasbley, A., Klotz, S., Triboulet, R. (1999) Synthesis and growth of PbTe crystals at low temperature and their characterization, *Journal of Crystal Growth*, 196 p. 71-76. [https://doi.org/10.1016/S0022-0248\(98\)00882-3](https://doi.org/10.1016/S0022-0248(98)00882-3)
- [4]. Ivanov, V.A., Gremenok, V. F., Seidi, H.G. (2013) Electrical Properties of Hot wall deposited PbTe-SnTe Thin Film, *Nanosystems: Physics, Chemistry, Mathematics*, 4 (6) p.816-822
- [5]. Alvi, M.A. and Khan, Z.H. (2013) Synthesis and Characterization of Nanoparticle Thin Films of $a\text{-(PbSe)}_{100-x}\text{Cd}_x$ Lead Chalcogenides, *Nanoscale Research Letters*, 8 (1) 148.
- [6]. Kungumadevi, L., Sathyamorthy, R. and Subbarayan, A. (2010) AC conductivity and dielectric properties of thermally evaporated PbTe thin films, *Solid State Electronics*, 54 p.58-62



- [7]. Kungumadevi, L. and Sathyamorthy, R. (2012) Advances in Condensed Matter Physics, 2012 (2012) ID 763209, 5 pages.
- [8]. Kumar, S., Khan, Z.H., Majeed Khan, M.A. and Husain, M. (2005) Studies on thin films of lead chalcogenides, Current Applied Physics, 5p. 561-566. <https://doi.org/10.1016/j.cap.2004.07.001>
- [9]. Delin, A., Ravindran, P., Eriksson, O. and Wills, J. M. (1998) Full potential optical calculations of lead chalcogenides, International Journal of Quantum Chemistry, 69 No. 3 p. 349-358.
- [10]. Gille, P. and Rudolph, P. (1983). Growth of Ti Doped PbTe Single Crystals By The Travelling Heater Method, Journal of Crystal Growth, 64 p. 613-614
- [11]. Sonia Gumaraes et al. (2002) Materials Research Society Symposium Proceedings, 692 (2002) p. 175-180.
- [12]. Chavez Urbiola, I.R., Bernel Martinez, J.A. et al. (2014) Combined CBD-CVD Technique for Preparation of II-VI Semiconductor Films for Solar Cells, Energy Procedia 57 p.24-31
- [13]. Chavez Urbiola, I.R., Bernel Martinez, J.A. et al. (2014) Preparation of II-VI and IV-VI semiconductor films for solar cells by the isovalent substitution technique with a CBD-made substrate, Inorganic Materials, 50 No.66 p.546-550
- [14]. Luther, J.M., Matt Law, Qing Song et al. (2008). Schottky Solar Cells Based on Colloidal Nanocrystal Films, American Chemical Society, 2 No. 2p.271-280 <https://doi.org/10.1021/nl802476m>
- [15]. Rogacheva, E.I., Grigorov, S.N. et al. (2005). Investigation of the growth mechanism, structure, and thermoelectric properties of thin PbTe films grown on mica, Functional Materials, 12 No. 1 p. 21-27
- [16]. Saloniemi, H., Kannian, T. et al. Thin Solid Films, 326 (1998) p. 78-82
- [17]. Dauscher, A. Dinescu, M. et al. (2006) Temperature-dependant growth of PbTe pulsed laser deposited films on various substrates, Thin Solid Films, 497 p.170-176. <https://doi.org/10.1016/j.tsf.2005.10.079>
- [18]. Abd EL-Ati, M. I. (1997) Electrical conductivity of PbTe thin films, Physics Solid State, 39(1) (1997) p.68-71.
- [19]. Wang, J., Hu, J. et al. Journal of Applied Physics, 104 (05) 3767 (2008) p. 1-5
- [20]. Zogg, H., Fach, A., Maissen, C., Masek, J. And Blumer, S. (1994) Optical Engineering, 33 (5) (1994) p. 1440-1449.
- [21]. Teichert, C., Jamnig, B. and Oswald, J. (2008): Pattern formation in PbTe multilayer films Surface Science, 454-456 p. 823-826.
- [22]. Baleva M. and Surtchev M. (2002) Structural and optical characterization of laser-deposited PbTe films on silicon substrates, Vacuum, 69, Issues 1-3, p.419-423 [doi.org/10.1016/S0042-207X\(02\)00368-8](https://doi.org/10.1016/S0042-207X(02)00368-8)
- [23]. HoSoonmin, Middle East Journal of Scientific Research, 23 (11) (2005) p.2695- 2699.
- [24]. Nguyen M.P., Froemel J., Hatayama S., Sutou Y., J. Koike et al, (2016) Structure and thermoelectric properties of PbTe films deposited by thermal evaporation method. Proceedings of the 2016 IEEE 16th International Conference on Nanotechnology (IEEE-NANO) Japan. DOI: 10.1109/NANO.2016.7751384
- [25]. Qin, F. and Singh, P. (2014) PbTe/CdTe superlattices on ITO and a solar cell made from CdTe/CdS 2014 Published in IEEE 40th Photovoltaic Specialist Conference (PVSC) IEEE, 978-1-4799-4398 P.1682-1686 DOI.10.1109/PVSC.2014.6925244 DOI.
- [26]. Musa, A. O. (2010) Principles of Photovoltaic Energy Conversion, ABU Press, Zaria (2010) 1ST Ed. P.
- [27]. Tamilselvani, V., Rahesh Kumar, R. and Narasimha Rao, K. Materials Letters, 96 (2013) p.162- 165.
- [28]. Pal, A. K., Mondal, A. And Chaudhuri, S. (1990) Preparation and characterization of ZnTe/CdSe solar cells, Vacuum, 41 Nos. 4-6 1460-1462. [https://doi.org/10.1016/0042-207X\(90\)93990-Z](https://doi.org/10.1016/0042-207X(90)93990-Z)
- [29]. Muthukumarasamy, N., Balasundara Prabhu, R., Jayakumar, S. And Kannan, M.D. (2007) Photoconductive properties of hot wall deposited CdSe_{0.6}Te_{0.4} thin films, Materials Science and Engineering, B 137 P.1-4. <https://doi.org/10.1016/j.mseb.2006.06.057>
- [30]. Arthi, A.P., Sumithra Devi, M. and Thamizharasan, K. (2014) Journal of Solid State Physics, ID 153272, 5 pages.



- [31]. De Laurentis, M. and Irace, A. (2014) Optical Measurement Techniques of Recombination Lifetime Based on the Free Carriers Absorption Effect, Journal of Solid State Physics, 19 pages. <https://doi.org/10.1155/2014/291469>
- [32]. Ahuome B. A., Adamu, I., Adamu, M. A. and Baba-Kutigi, A. N. (2019) Growth and Characterization of PbTe Thin-film through Solvo Thermal Method, Physical Science International Journal 22(2) p.1-5, Article no.PSIJ.48981, ISSN: 2348-0130. DOI:10.9734/PSIJ/2019/v22i230126
- [33]. Perdew J. P., Burke, K., Ernzerhof, M. (1997) Generalized gradient approximation made simple. Phys. Rev. Letter. 1997;77(18):231–242. 3865–3868.
- [34]. Parr R. G. and Yang W. (1989). *Density-Functional Theory of Atoms and Molecules*. Oxford University Press: New York.
- [35]. Cohen, M.L. and Chelikowsky, J.R. (1988) Electronic Structure and Optical Properties of Semiconductors, Springer-Verlag, Berlin, 264 p. <http://dx.doi.org/10.1007/978-3-642-97080-1>.
- [36]. Semiconductors: Group IV Elements, IV-IV and III-IV Compounds, Landolt-Börnstein, New Series, Group III, Vol. 41, Pt. A, edited by O. Madelung, U. Rössler, and M. Schulz SpringerVerlag, Berlin, 2005.

